Longitudinal polarization of hyperon and antihyperon in semi-inclusive deep-inelastic scattering

Shan-shan Zhou, Ye Chen, Zuo-tang Liang, and Qing-hua Xu
School of Physics, Shandong University, Jinan, Shandong 250100, China
(Received 12 February 2009; published 19 May 2009)

We make a detailed study of the longitudinal polarization of hyperons and antihyperons in semi-inclusive deep-inelastic lepton-nucleon scattering. We present the numerical results for spin transfer in quark fragmentation processes, and analyze the possible origins for a difference between the polarization for hyperon and that for the corresponding antihyperon. We present the results obtained in the case that there is no asymmetry between sea and antisea distribution in the nucleon as well as those obtained when such an asymmetry is taken into account. We compare the results with the available data such as those from COMPASS and make predictions for future experiments including those at even higher energies such as at eRHIC.

DOI: 10.1103/PhysRevD.79.094018 PACS numbers: 13.88.+e, 13.60.−r, 13.85.Ni, 13.87.Fh

I. INTRODUCTION

Because of the nonperturbative nature, our knowledge on hadron structure and that on the fragmentation function are still very much limited, in particular in the polarized case. Deeply inelastic lepton-nucleon scattering is always an ideal place for such study because, at sufficiently high energy and momentum transfer, the factorization theorem is applicable and the hard part is easy to be calculated. Hyperon polarizations have been widely used for such studies, since they can easily be determined by measuring the angular distributions of the decay products. These studies have attracted much attention in past years [see e.g., [1–28]]. Longitudinal polarizations of hyperons and antihyperons in semi-inclusive deep-inelastic scattering (SIDIS) have been studied both experimentally and theoretically. More recently, such studies have, in particular, been extended to antihyperons. Special attention is paid to the comparison of the results for hyperons with those for the corresponding antihyperons. This is partly triggered by the results of COMPASS collaboration at CERN which seem to tell us that there is a difference between Λ and $\bar{\Lambda}$ polarization in semi-inclusive deep-inelastic lepton-nucleon scattering [6,7]. A detailed study of such a difference can provide us useful information on the polarized fragmentation function and the structure of the nucleon sea. It might be considered as a signature of the existence of a difference between the strange sea and antisea distributions in nucleon as proposed in literature some time ago [29–36]. It could also be a signature for a difference between the spin transfer in quark and antiquark fragmentation. On the other hand, it is also clear that the valence quarks in nucleon and other known effects can also contribute to such a difference. It is therefore important to make a detailed and systematic analysis of the contributions from such known effects before we extract information on the possible asymmetry between sea and antisea distributions.

In this paper, we make such a systematic study of longitudinal polarization of different hyperons and antihyperons in semi-inclusive deep-inelastic lepton-nucleon scattering. We make a detailed analysis on the possible origin(s) of the difference between hyperon and antihyperon polarization at COMPASS and even higher energies. We clarify the different contributions and present the results obtained in the case that there is no asymmetry between nucleon sea and antisea quark distributions as well as those obtained when such an asymmetry is taken into account. We make the calculations not only for Λ and $\bar{\Lambda}$ but also other hyperons and antihyperons in the same $J^P = (1/2)^+$ octet. We compare our results with the available data and make predictions for future experiments, in particular at eRHIC [37]. These results can serve as a guide to study the polarized fragmentation functions and will, in particular, show whether, if yes how, a significant difference between sea and antisea quark distribution in the nucleon can manifest itself in a difference between the polarization of hyperon and that of the corresponding antihyperon in SIDIS with a longitudinally polarized beam.

The paper is organized as follows: After this Introduction, in Sec. II, we summarize the general framework for the calculations of the longitudinal polarization P_H of the hyperon H and $P_{\bar{H}}$ of the antihyperon $\bar{H}$ based on factorization theorem, and make a detailed analysis of each factor used in the formulas. We present, in particular, the model calculation results for spin transfer for a pure quark fragmentation process and compare the results for hyperons with those for antihyperons. In Sec. III, we present the results obtained for hyperon and antihyperon polarizations in reactions using polarized beam and unpolarized target for the case that there is no asymmetry between the sea and antisea distributions in the nucleon and those for the case that such an asymmetry is taken into account. We also study the influence from the differences in quark distributions as given by different sets of parame-

trizations. In Sec. IV, we study the case that the lepton beam is unpolarized but the nucleon is polarized and present the results obtained using different parametrizations of the polarized parton distributions. Finally, in Sec. V, we give a short summary and discussion.

II. GENERAL FRAMEWORK FOR CALCULATING P_H AND $P_{\bar{H}}$ IN SIDIS

Deeply inelastic lepton-nucleon scattering at sufficiently high energy and momentum transfer is one of the places where factorization theorem is applicable and is tested with high accuracies. According to the factorization theorem, hadron production in the current fragmentation region of SIDIS is a pure result of the fragmentation of the quark or antiquark scattered by the incoming lepton. The cross section is given as a convolution of quark distribution function in the nucleon, the elementary lepton-parton scattering, and the fragmentation function. We consider the longitudinally polarized reaction in this paper and, for definiteness, we consider $e^- + N \to e^- + H(\text{or } \bar{H}) + X$ as an example. The formulas can be extended to other reactions in a straightforward way. To the leading order in perturbation theory, the differential cross section for $e^- + N \to e^- + H + X$ is given by

$$d\sigma_{\lambda_H;\lambda_e,\lambda_N} = \sum_{f,\lambda_f} \int dxdydzK(x,y)[q^{N,\lambda_N}_{f,\lambda_f}(x) d\hat{\sigma}^{eq}_{\lambda_e,\lambda_f}(x,y) \times D^{H,\lambda_H}_{f,\lambda_f}(z) + (q_f \leftrightarrow \bar{q}_f)], \quad (1)$$

where λ_e, λ_N, λ_f, and λ_H are, respectively, the helicities of the electron, the incoming nucleon, the struck quark q_f, and the produced hyperon H; x is the usual Bjorken-x, y is the fractional energy transfer from the electron to the nucleon N in the rest frame of N; z is the fraction of momentum of scattered q_f carried by the produced hyperon H; and $K(x, y)$ is a kinematic factor which contains the $1/Q^4$ due to the photon propagator and others ($Q^2 = -q^2$ and q is the four momentum transfer). The sum over f runs over all the different flavor of quarks or antiquarks. Here, for clarity, we did not write out the scale dependence of the parton distributions and fragmentation functions explicitly. They are understood implicitly. We consider only light quarks and antiquarks. Hence, both quark and electron mass are neglected so that helicity in the elementary scattering process $eq \to eq$ is conserved.

Equation (1) is the basis for calculating the cross section of SIDIS both in the unpolarized and the polarized case. We use this formula as the starting point for calculating the polarizations of hyperons and antihyperons in SIDIS in the following but discuss possible violation effects in Sec. II F.

A. The calculation formulas for P_H and $P_{\bar{H}}$

The polarization of H in $e^- + N \to e^- + H(\text{or } \bar{H}) + X$ is usually defined as

$$P_H(z) \equiv \frac{d\sigma_{+;\lambda_e\lambda_N} - d\sigma_{-;\lambda_e\lambda_N}}{d\sigma_{+;\lambda_e\lambda_N} + d\sigma_{-;\lambda_e\lambda_N}}, \quad (2)$$

for the case that both the beam and target are completely polarized in the pure states with helicities λ_e and λ_N. In the case that factorization theorem is valid, we can just insert Eq. (1) into Eq. (2) and obtain the result for the polarization of hyperon in $e^- + p \to e^- + H + X$ with longitudinally polarized electron beam and proton target as

$$P_H(z) = \frac{\sum_f e_f^2 \int dxdyK(x,y)\{P_f(x,y)[q_f(x) + P_b P_T D_L(y)\Delta q_f(x)]\Delta D_f^H(z) + (q_f \leftrightarrow \bar{q}_f)\}}{\sum_f e_f^2 \int dxdyK(x,y)\{[q_f(x) + P_b P_T D_L(y)\Delta q_f(x)] D_f^H(z) + (q_f \leftrightarrow \bar{q}_f)\}}, \quad (3)$$

where P_b and P_T denote the longitudinal polarization of the electron beam and nucleon target, respectively; e_f is the electric charge of quark q_f, $q_f(x)$ and $\Delta q_f(x)$ are the unpolarized and polarized quark distribution functions, $P_f(x, y)$ is the polarization of the scattered quark q_f, $D_L(y)$ is the longitudinal spin transfer factor in the elementary scattering process $eq \to eq$ and is defined as

$$D_L(y) \equiv \frac{d\hat{\sigma}^{eq}_{++} - d\hat{\sigma}^{eq}_{+-}}{d\hat{\sigma}^{eq}_{++} + d\hat{\sigma}^{eq}_{+-}}, \quad (4)$$

which is only a function of y at the leading order in perturbative QED; $D_f^H(z)$ and $\Delta D_f^H(z)$ are the unpolarized and polarized fragmentation functions that are defined as

$$D_f^H(z) \equiv D_f^H(z,+) + D_f^H(z,-), \quad (5)$$

$$\Delta D_f^H(z) \equiv D_f^H(z,+) - D_f^H(z,-), \quad (6)$$

where the argument $+$ or $-$ denotes that the helicity of the produced hyperon H is the same as or opposite to that of the fragmenting q_f. In the notation used in Eq. (1), they are $D_f^H(z,+) = D^{H,+}_{f,+}(z) = D^{H,-}_{f,-}(z)$ and $D_f^H(z,-) = D^{H,+}_{f,-}(z) = D^{H,-}_{f,+}(z)$. The integrations over x and y run over the kinematic region determined by the corresponding experiments.

Similarly for antihyperon $\bar{H}$ in $e^- + p \to e^- + \bar{H} + X$, the polarization is given by

$$P_{\bar{H}}(z) = \frac{\sum_f e_f^2 \int dxdyK(x,y)\{P_f(x,y)[q_f(x) + P_b P_T D_L(y)\Delta q_f(x)]\Delta D_f^{\bar{H}}(z) + (q_f \leftrightarrow \bar{q}_f)\}}{\sum_f e_f^2 \int dxdyK(x,y)\{[q_f(x) + P_b P_T D_L(y)\Delta q_f(x)]D_f^{\bar{H}}(z) + (q_f \leftrightarrow \bar{q}_f)\}}. \quad (7)$$

The physical significance of the expressions in Eqs. (3) and (7) is very clear: In the denominator, besides some kinematic factor, we have just the production rate of H or $\bar{H}$. The appearance of the term proportional to $P_b P_T$ is due to the double spin asymmetry $\hat{a}_{LL}$ in the elementary scattering process $eq \to eq$ which measures the difference between $\hat{\sigma}^{eq}_{++}$ and $\hat{\sigma}^{eq}_{+-}$. The numerator shows explicitly that the polarization of H or $\bar{H}$ just comes from that of the q_f and/or $\bar{q}_f$ after the eq scattering. This can be seen more clearly if we rewrite Eqs. (3) and (7) as

$$P_H(z) = \sum_f \int dxdy[P_f(x,y)R_f^H(x,y,z|\text{pol})S_f^H(z) + (q_f \leftrightarrow \bar{q}_f)], \quad (8)$$

$$P_{\bar{H}}(z) = \sum_f \int dxdy[P_f(x,y)R_f^{\bar{H}}(x,y,z|\text{pol})S_f^{\bar{H}}(z) + (q_f \leftrightarrow \bar{q}_f)], \quad (9)$$

where $R_f^H(x,y,z|\text{pol})$ is the fractional contribution from q_f to the production of H in $e^- + p \to e^- + H + X$ and is given by

$$R_f^H(x,y,z|\text{pol}) = \frac{e_f^2 K(x,y)[q_f(x) + P_b P_T D_L(y)\Delta q_f(x)]D_f^H(z)}{\sum_f e_f^2 \int dxdyK(x,y)\{[q_f(x) + P_b P_T D_L(y)\Delta q_f(x)]D_f^H(z) + (q_f \leftrightarrow \bar{q}_f)\}}; \quad (10)$$

$S_f^H(z)$ is the polarization transfer in the fragmentation process $q_f \to H + X$ in the longitudinally polarized case and is defined as

$$S_f^H(z) \equiv \Delta D_f^H(z)/D_f^H(z). \quad (11)$$

We see that the polarization of H or $\bar{H}$, $P_H(z)$ or $P_{\bar{H}}(z)$, is just a weighted sum of $S_f^H(z)$ and $S_{\bar{f}}^H(z)$ for different flavor f. The weights are products of $P_f(x,y)$, the polarization of quark after the elementary scattering, and $R_f^H(x,y,z|\text{pol})$, the fractional contribution from q_f to the production of H. In fact, assuming the validity of factorization theorem, fragmentation functions should be universal so that $S_f^H(z)$ and $S_{\bar{f}}^H(z)$ are also universal. Different results for $P_H(z)$ in different kinematic regions and/or different reactions just originate from the differences in $P_f(x,y)$ and $R_f^H(x,y,z|\text{pol})$.

The expression for the relative weight $R_f^H(x,y,z|\text{pol})$ is much simpler if we have only beam or target polarized, i.e., we have either $P_T = 0$ or $P_b = 0$. In this case, the term proportional to $P_b P_T$ vanishes and we have $R_f^H(x,y,z|\text{pol})|_{P_b=0} = R_f^H(x,y,z|\text{pol})|_{P_T=0} = R_f^H(x,y,z|\text{unpol})$, which we simply denote by $R_f^H(x,y,z)$ and is given by

$$R_f^H(x,y,z) = \frac{e_f^2 K(x,y)q_f(x)D_f^H(z)}{\sum_f e_f^2 \int dxdyK(x,y)[q_f(x)D_f^H(z) + \bar{q}_f(x)D_{\bar{f}}^H(z)]}. \quad (12)$$

We see that $R_f^H(x,y,z)$ is determined solely by the unpolarized quantities such as the unpolarized parton distributions and fragmentation functions.

The quark polarization is determined by the initial quark and/or electron polarization and the spin transfer in the elementary process. It is given by

$$P_f(x,y) = \frac{P_b D_L(y)q_f(x) + P_T\Delta q_f(x)}{q_f(x) + P_b D_L(y)P_T\Delta q_f(x)}, \quad (13)$$

$$P_{\bar{f}}(x,y) = \frac{P_b D_L(y)\bar{q}_f(x) + P_T\Delta \bar{q}_f(x)}{\bar{q}_f(x) + P_b D_L(y)P_T\Delta \bar{q}_f(x)}, \quad (14)$$

where the longitudinal spin transfer factor $D_L(y)$ in $eq \to eq$ can be obtained using perturbative QED and, to the leading order, is the same for $eq \to eq$ and $e\bar{q} \to e\bar{q}$ and is given by

$$D_L(y) = \frac{1-(1-y)^2}{1+(1-y)^2}, \quad (15)$$

which is positive for $0 < y < 1$, it equals to 0 for $y = 0$, increases monotonically with increasing y and reaches 1 at $y = 1$.

The results in Eqs. (13) and (14) have the following features.

(1) If the target is unpolarized, i.e. $P_T = 0$ but $P_b \neq 0$, we have

$$P_f(x, y|P_T = 0) = P_{\bar{f}}(x, y|P_T = 0) = P_b D_L(y), \quad (16)$$

which is only a function of y and is the same not only for different flavors but also for quark and antiquark. We see that the quark (antiquark) polarization in this case is completely known. This is a very good place to study the spin transfer in fragmentation and/or the factors contained in the fractional contributions to the production of H and $\bar{H}$. The expression for hyperon polarization in this case becomes also simpler. It is given by

$$P_H(z|P_T = 0) = \int dxdy P_b D_L(y) \sum_f [R_f^H(x, y, z) S_f^H(z) + R_{\bar{f}}^H(x, y, z) S_{\bar{f}}^H(z)], \quad (17)$$

$$P_{\bar{H}}(z|P_T = 0) = \int dxdy P_b D_L(y) \sum_f [R_f^{\bar{H}}(x, y, z) S_f^{\bar{H}}(z) + R_{\bar{f}}^{\bar{H}}(x, y, z) S_{\bar{f}}^{\bar{H}}(z)]. \quad (18)$$

For a fixed value of y, we have

$$P_H(z, y|P_T = 0) = \int dx P_b D_L(y) \sum_f [R_{fy}^H(x, y, z) S_f^H(z) + R_{\bar{f}y}^H(x, y, z) S_{\bar{f}}^H(z)], \quad (19)$$

$$R_{fy}^H(x, y, z) = \frac{e_f^2 K(x, y) q_f(x) D_f^H(z)}{\sum_f e_f^2 \int dx K(x, y)[q_f(x) D_f^H(z) + \bar{q}_f(x) D_{\bar{f}}^H(z)]}. \quad (20)$$

If we now define $S_{ep}^H(z, y) \equiv P_H(z, y|P_T = 0)/P_b D_L(y)$ as in COMPASS measurements [6,7], we obtain that

$$S_{ep}^H(z, y) = \sum_f \int dx [R_{fy}^H(x, y, z) S_f^H(z) + R_{\bar{f}y}^H(x, y, z) S_{\bar{f}}^H(z)]. \quad (21)$$

We see that $S_{ep}^H(z, y)$ is just a weighted sum of $S_f^H(z)$ and $S_{\bar{f}}^H(z)$, and the weights are determined by unpolarized quantities. Denote

$$\langle R_{fy}^H(y, z)\rangle \equiv \int dx R_{fy}^H(x, y, z) = \frac{e_f^2 \int dx K(x, y) q_f(x) D_f^H(z)}{\sum_f e_f^2 \int dx K(x, y)[q_f(x) D_f^H(z) + \bar{q}_f(x) D_{\bar{f}}^H(z)]}, \quad (22)$$

and we obtain

$$S_{ep}^H(z, y) = \sum_f [\langle R_{fy}^H(y, z)\rangle S_f^H(z) + \langle R_{\bar{f}y}^H(y, z)\rangle S_{\bar{f}}^H(z)]. \quad (23)$$

In practice, one often deals with events in a given y interval, and one has

$$S_{ep}^H(z) = \sum_f [\langle R_{fy\text{int}}^H(z)\rangle S_f^H(z) + \langle R_{\bar{f}y\text{int}}^H(z)\rangle S_{\bar{f}}^H(z)], \quad (24)$$

$$\langle R_{fy\text{int}}^H(z)\rangle = \frac{e_f^2 \int dxdy K(x, y) q_f(x) D_f^H(z)}{\sum_f e_f^2 \int dxdy K(x, y)[q_f(x) D_f^H(z) + \bar{q}_f(x) D_{\bar{f}}^H(z)]}. \quad (25)$$

(2) If the beam is unpolarized but the target is polarized, i.e. $P_b = 0$ but $P_T \neq 0$, we have

$$P_f(x, y|P_b = 0) = P_T \Delta q_f(x)/q_f(x), \quad (26)$$

$$P_{\bar{f}}(x, y|P_b = 0) = P_T \Delta \bar{q}_f(x)/\bar{q}_f(x), \quad (27)$$

which is nothing else but the quark polarization before the eq scattering. This is just a result of helicity conservation. In this case, we have

$$P_H(z|P_b=0)=\frac{\sum_f e_f^2 P_T \int dxdyK(x,y)[\Delta q_f(x)\Delta D_f^H(z)+\Delta\bar{q}_f(x)\Delta D_{\bar{f}}^H(z)]}{\sum_f e_f^2 \int dxdyK(x,y)[q_f(x)D_f^H(z)+\bar{q}_f(x)D_{\bar{f}}^H(z)]}, \tag{28}$$

where the polarizations of hyperons and antihyperons are determined by the polarizations of quarks and antiquarks in nucleon, thus can be used to extract information on the polarized quark distributions in nucleon.

(3) In the case that neither P_b nor P_T is zero, i.e. both electron beam and nucleon target are polarized, the polarization of q_f or $\bar{q}_f$ after the scattering with electron is mainly determined by the beam electron polarization. It is dominated by the spin transfer from the electron to the scattered quark (antiquark). The influence from the target polarization is relatively small. Aiming at studying either fragmentation functions or quark distributions, this case does not have much advantage compared to the cases (1) and (2) mentioned above. We therefore concentrate on the cases (1) and (2) in the following text of this paper.

From the discussions presented above, we see that there are three factors, i.e., quark polarization, the relative weights, and the fragmentation function are involved in Eqs. (8)–(11) for final hyperon or antihyperon polarization. We now discuss them further separately in the following.

B. The spin transfer factor $D_L(y)$ in $eq \to eq$ scattering

This is one of the best known factors involved in Eqs. (3) and (7). Since it is determined mainly by the electromagnetic interaction, the spin transfer factor $D_L(y)$ in $eq \to eq$ scattering is calculable using perturbation theory in QED. When next-leading order effects are taken into account, perturbative QCD (pQCD) corrections are involved. The result given in Eq. (15) is obtained at leading order in perturbation theory. In this case, $D_L(y)$ is the same for quark and antiquark, i.e.,

$$D_L^{eq\to eq}(y)=D_L^{e\bar{q}\to e\bar{q}}(y). \tag{29}$$

It is also the same for electron or positron. However, if we consider next-leading order in QED, e.g., if we take two photon exchange into account, the interference term leads to a difference between quark and antiquark. It is also obvious that next-leading order in QED is far away from influencing the results at the accuracies of the data available. We consider only the leading order here.

Similarly, we also stick to leading order in perturbative QCD. The next-to-leading order calculations are in principle straightforward but much involved (see e.g. [38]). These results should be used consistently with the polarized parton distributions functions and the polarized fragmentation functions. In view of our current knowledge on the polarized fragmentation functions, we consider only the leading order consistently in this paper.

C. The relative weights and the parton distributions

Using charge conjugation symmetry for the fragmentation functions, we have

$$R_{\bar{f}}^{\bar{H}}(x,y,z)=\frac{e_f^2 K(x,y)\bar{q}_f(x)D_f^H(z)}{\sum_f e_f^2 \int dxdyK(x,y)[\bar{q}_f(x)D_f^H(z)+q_f(x)D_{\bar{f}}^H(z)]}. \tag{30}$$

This is to compare with $R_f^H(x,y,z)$ given in Eq. (12). We see that the difference between $q_f(x)$ and $\bar{q}_f(x)$ is the only source for the difference between $R_f^H(x,y,z)$ and $R_{\bar{f}}^{\bar{H}}(x,y,z)$.

One obvious source for the difference between $q_f(x)$ and $\bar{q}_f(x)$ is the valence quark contribution. Although this influences only u and d, it makes the ratio of the contributions from u, d, and s to H different from the corresponding ratio for the contributions from $\bar{u}$, $\bar{d}$, and $\bar{s}$ to $\bar{H}$. As we will see clearly from Fig. 2 in the next subsection, S_f^H is very much different for different f, and such a different ratio leads to different P_H and $P_{\bar{H}}$.

Clearly, valence quark contributions are negligible at very small x. We therefore expect that its influence becomes negligible at very high energies. Also, since the influence is determined by the ratio of $u(x)$, $d(x)$ and $s(x)$, the results can be quite sensitive to the forms of the parton distributions.

The unpolarized parton distribution functions $q_f(x)$ are determined from unpolarized deep-inelastic scattering and other related data from unpolarized experiments. There are different sets available in the parton distribution function library (PDFLIB [39]) package. Although the qualitative features are all the same, there are differences in the fine structure, which may influence the difference between $R_f^H(x,y,z)$ and $R_{\bar{f}}^{\bar{H}}(x,y,z)$ and lead to different results in P_H and $P_{\bar{H}}$. We will study this in the next sections.

Another source of the difference between $q_f(x)$ and $\bar{q}_f(x)$ is the asymmetry in nucleon sea and antisea distributions. The physical picture for such an asymmetry was proposed [29–34] and models or parametrizations exist [35,36]. This should be the dominant source for the difference between $q_f(x)$ and $\bar{q}_f(x)$ at very small x and can be better studied at higher energies if it indeed leads to a significant difference between $R_f^H(x,y,z)$ and $R_{\bar{f}}^{\bar{H}}(x,y,z)$

thus a significant difference between $P_H(z)$ and $P_{\bar{H}}(z)$. We will also make calculations for this case in Sec. III.

D. Spin transfer in fragmentation process

Spin transfer in fragmentation is defined in Eq. (11) and is given by the polarized fragmentation functions $\Delta D_f^H(z)$. For explicitly, we only consider the fragmentation process $q_f \to H + X$. We should note that, when writing the factorization theorem in the way as given in Eq. (1), we assume that the fragmentation function is defined inclusively for the fragmentation process $q_f \to H + X$. It should include all the contributions from all the decay processes including strong as well as other decay processes. However, to study the physics behind it, it is useful to divide it into the directly produced part and the decay contributions. It has been widely used in studying the fragmentation functions in unpolarized processes and has been outlined in different publications [11–18]. Here, for completeness, we summarize the major equations in the following.

According to this classification, we write

$$D_f^H(z) = D_f^H(z;\mathrm{dir}) + D_f^H(z;\mathrm{dec}), \tag{31}$$

where the $D_f^H(z;\mathrm{dir})$ and $D_f^H(z;\mathrm{dec})$ are the directly produced and decay contribution part, respectively. The decay contribution can be calculated by

$$D_f^H(z;\mathrm{dec}) = \sum_j \int dz' K_{H,H_j}(z,z') D_f^{H_j}(z'), \tag{32}$$

where the kernel function $K_{H,H_j}(z,z')$ is the probability for H_j with the fractional momentum z' to decay into a H with fractional momentum z, and, e.g., for a two body decay $H_j \to H + M$, it is given by

$$K_{H,H_j}(z,z') = \frac{N}{E_j}\mathrm{Br}(H_j \to H + M)\delta(p.p_j - m_j E^*), \tag{33}$$

where $\mathrm{Br}(H_j \to H + M)$ is the decay branching ratio, N is the normalization constant, and E^* is the energy of H in the rest frame of H_j, and m_j is the mass of H_j.

Similarly, in the polarized case, we have

$$\Delta D_f^H(z) = \Delta D_f^H(z;\mathrm{dir}) + \Delta D_f^H(z;\mathrm{dec}), \tag{34}$$

and the decay part is given by

$$\Delta D_f^H(z;\mathrm{dec}) = \sum_j \int dz' t_{H,H_j}^D K_{H,H_j}(z,z') \Delta D_f^{H_j}(z'), \tag{35}$$

where t_{H,H_j}^D is a constant called the decay spin transfer which is independent of the H_j produced process, and is e.g. discussed and given in Table 2 of Ref. [11].

We should note that, in Eqs. (32) and (35), when calculating different decay contributions, we have added the contributions from different hyperon decays incoherently. This is what one often does in calculating inclusive quantities where the interferences are usually small because of the small contributions from different channels to exactly the same final state at exactly the same phase space points.

1. Modeling $\Delta D_f^H(z, \mathbf{dir})$

Since fragmentation is a nonperturbative process, the fragmentation function cannot be calculated using perturbative QCD. At present, we have to invoke parametrization and/or phenomenological models. There are already data available [1–8] that can be used to extract information on the polarized fragmentation functions $\Delta D_f^H(z, \mathrm{dir})$ but still far away from giving a good control of the form of it. At this stage, phenomenological models are quite useful, in particular, in obtaining some guide for experiments. In this connection, the model invoking calculation method according to the origins of hyperon is very practical and successful [9–18]. In this model, one classifies the directly produced hyperons into the following two categories: (A) those which contain the initial quark q_f and (B) those which do not contain the initial quark, i.e.,

$$D_f^H(z;\mathrm{dir}) = D_f^{H(A)}(z) + D_f^{H(B)}(z), \tag{36}$$

$$\Delta D_f^H(z;\mathrm{dir}) = \Delta D_f^{H(A)}(z) + \Delta D_f^{H(B)}(z). \tag{37}$$

It is assumed that those do not contain the initial quark are unpolarized, so that

$$\Delta D_f^{H(B)}(z) = 0. \tag{38}$$

The polarization then originates only from category (A) and is given by

$$\Delta D_f^{H(A)}(z) = t_{H,f}^F D_f^{H(A)}(z), \tag{39}$$

in which $t_{H,f}^F$ is known as the fragmentation spin transfer factor and is taken as a constant given by

$$t_{H,f}^F = \Delta Q_f / n_f, \tag{40}$$

where ΔQ_f is the fractional spin contribution of a quark with flavor f to the spin of the hyperon, and n_f is the number of valence quarks of flavor f in H.

The model is very practical and useful for the following reason: In the recursive cascade hadronization models, such as Feynman-Field–type fragmentation models [40] where a simple elementary process takes place recursively, $D_f^{H(A)}(z)$ and $D_f^{H(B)}(z)$ are well defined and determined. In such models, $D_f^{H(A)}(z)$ is the probability to produce a first rank H which is usually denoted by $f_{q_f}^H(z)$ and is well determined by unpolarized reaction data. Hence, the z dependence ΔD given above is obtained completely from the unpolarized fragmentation functions, which are empirically known. The only unknown is the spin transfer constant $t_{H,f}^F = \Delta Q_f / n_f$. By using either the SU(6) wave

function or polarized deep-inelastic lepton-nucleon scattering data, one obtains two distinct expectations ΔQ_f, the so-called SU(6) and DIS expectations, see Table 1 of [11].

This approach has been applied to different hyperons/antihyperons in different reactions such as e^+e^-, SIDIS and pp collisions [9–18] and compared with data [1–8]. The current experimental accuracy does not allow one to distinguish between the expectations for $t^F_{H,f}$ based on the SU(6) and DIS pictures. However, the z dependence of the available data on Λ polarization is well described [11].

2. *Numerical results for* $S^H_f(z)$

Using the definition given in Eq. (11) and (34), we obtain the spin transfer for $q_f \to H + X$ as

$$S^H_f(z) = S^H_f(z, \text{dir}) + S^H_f(z, \text{dec}). \tag{41}$$

In the model described above, we have

$$S^H_f(z, \text{dir}) = t^F_{H,f} A^H_f(z, \text{dir}), \tag{42}$$

$$A^H_f(z, \text{dir}) = f^H_{q_f}(z)/D^H_f(z). \tag{43}$$

If we do not consider successive decay, we have

$$S^H_f(z, \text{dec}) = \sum_j t^F_{H_j,f} t^D_{H,H_j} A^H_{f,H_j}(z, \text{dec}), \tag{44}$$

$$A^H_{f,H_j}(z, \text{dec}) = \int dz' K_{H,H_j}(z, z') f^{H_j}_{q_f}(z')/D^H_f(z). \tag{45}$$

We call $A^H_f(z, \text{dir})$ and $A^H_{f,H_j}(z, \text{dec})$ first rank contributions and note that both of them are determined by the unpolarized fragmentation functions. As an example, we calculated them using Lund fragmentation model [41] as implemented in the Monte-Carlo event generator PYTHIA [42]. The results are given in Fig. 1. Because isospin symmetry is valid here, so we have relations such as $A^\Lambda_u(z, \text{dir}) = A^\Lambda_d(z, \text{dir})$, $A^{\Sigma^+}_u(z, \text{dir}) = A^{\Sigma^-}_d(z, \text{dir})$, $A^{\Xi^0}_u(z, \text{dir}) = A^{\Xi^-}_d(z, \text{dir})$, etc. Hence, we only show the u and s contributions to Λ, Σ^+, and Ξ^0. All the others from u, d, and s quark to the $J^P = (1/2)^+$ hyperons can be obtained using such relations. We see, first of all, that the decay contributions to Λ are large but those to Σ and Ξ are negligible. We also see that s-quark contributions are large in general because those from u or d have strangeness suppression, a well-known factor in fragmentation process.

Multiplying by the corresponding spin transfer factors $t^F_{H,f}$ and t^D_{H,H_j}, we obtain the corresponding $S^H_f(z)$ as shown in Fig. 2.

We see that, for different flavors, $S^H_f(z)$ differs very much from each other not only because of the difference in the first rank contributions as shown in Fig. 1, but also because of the differences in the spin transfer factors $t^F_{H,f}$ and t^D_{H,H_j}. As an example, we see $S^{\Sigma^+}_u$ is positive and large while $S^{\Sigma^+}_s$ is negative and the magnitude is smaller than $S^{\Sigma^+}_u$. We also note that isospin symmetry is valid here so that we have a series of relations such as $S^\Lambda_u(z) = S^\Lambda_d(z)$, $S^{\Sigma^+}_u(z) = S^{\Sigma^-}_d(z)$, $S^{\Xi^0}_u(z) = S^{\Xi^-}_d(z)$, $S^{\Sigma^+}_s(z) = S^{\Sigma^-}_s(z)$, and $S^{\Xi^0}_s(z) = S^{\Xi^-}_s(z)$.

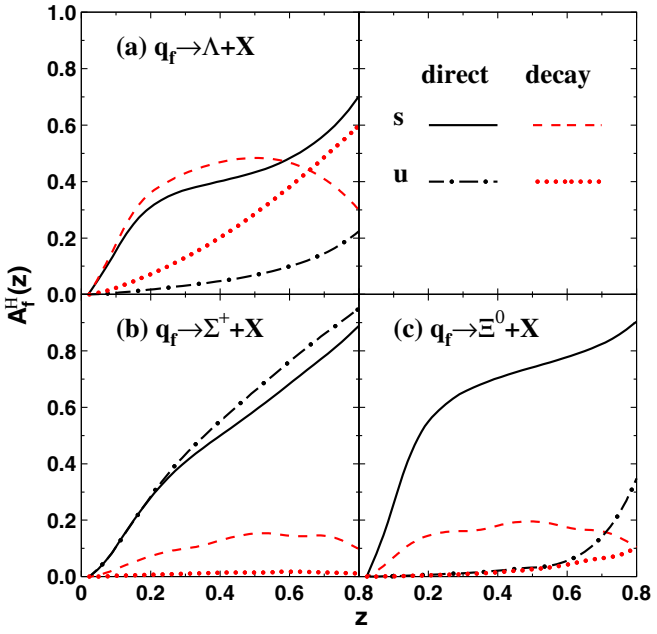

FIG. 1 (color online). First rank contributions $A^H_f(z, \text{dir})$ and $A^H_f(z, \text{dec})$ in quark fragmentation to the productions of different hyperons as the functions of z. The results are extracted from the e^+e^- process with $\sqrt{s} = 200$ GeV using PYTHIA.

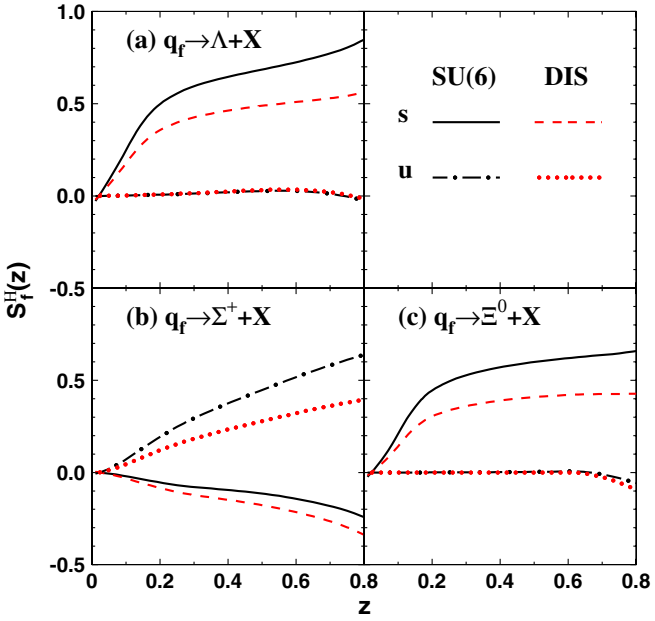

FIG. 2 (color online). Spin transfer $S^H_f(z)$ in the fragmentation process $q_f \to H + X$.

3. Comparing $S_f^H(z)$ with $S_{\bar{f}}^{\bar{H}}(z)$

For the fragmentation function, the directly produced part is controlled by strong interaction where charge conjugation symmetry is valid. Hence, we have

$$D_f^H(z, \text{dir}) = D_{\bar{f}}^{\bar{H}}(z, \text{dir}), \tag{46}$$

$$\Delta D_f^H(z, \text{dir}) = \Delta D_{\bar{f}}^{\bar{H}}(z, \text{dir}). \tag{47}$$

For the decay contributions, we have processes controlled by strong or electromagnetic interactions. In these processes, we still have charge conjugation symmetry so that similar equations as given above are valid. However, there are also weak decay processes that play a role. In a weak process, charge conjugation symmetry may be violated. There are a few weak decay processes that we need to take into account and we can check them one by one. Fortunately, for all the weak decay processes that give significant contribution to the production of hyperons (antihyperons) in our interest, no significant violation in charge conjugation symmetry has been observed. We therefore neglect the influence and have approximately that

$$D_f^H(z) = D_{\bar{f}}^{\bar{H}}(z), \tag{48}$$

$$\Delta D_f^H(z) = \Delta D_{\bar{f}}^{\bar{H}}(z), \tag{49}$$

We thus also have

$$S_f^H(z) = S_{\bar{f}}^{\bar{H}}(z), \tag{50}$$

$$S_{\bar{f}}^H(z) = S_f^{\bar{H}}(z). \tag{51}$$

We see, under such circumstances, we expect no significant difference between the spin transfer in quark fragmentation and that in antiquark fragmentation. A significant difference between final hyperon and antihyperon polarization can only be from the difference between $P_f(x, y)$ and $P_{\bar{f}}(x, y)$ and/or that between $R_f^H(x, y, z)$ and $R_{\bar{f}}^{\bar{H}}(x, y, z)$. We recall that, in the case of $P_T = 0$, $P_f(x, y|P_T = 0) = P_{\bar{f}}(x, y|P_T = 0) = P_b D_L(y)$, the only source for such a difference is the difference between $R_f^H(x, y, z)$ and $R_{\bar{f}}^{\bar{H}}(x, y, z)$, which we discussed in Sec. II C.

As an example, we see that, in the model described in Sec. II D 2,

$$S_{\bar{f}}^H(z) = S_f^{\bar{H}}(z) = 0, \tag{52}$$

$$S_f^H(z) = S_{\bar{f}}^{\bar{H}}(z) = t_{H,f}^F A_f^H(z, \text{dir}) + \sum_j t_{H_j,f}^F t_{H,H_j}^D A_{f,H_j}^H(z, \text{dec}). \tag{53}$$

Charge conjugation symmetry is indeed valid here and the numerical results are given in Fig. 2. We emphasize here that, as can be seen from Fig. 2, for different flavor f, $S_f^H(z)$ differs very much from each other. This makes the value of the polarization of final hyperon sensitive to $R_f^H(x, y, z)$. Hence, measuring P_H is a good way to study the fine behavior of $R_f^H(x, y, z)$.

E. A practical way of the calculations

As shown by Eqs. (8)–(10), the calculations of P_H and/or $P_{\bar{H}}$ involve the contributions from different flavor f and $\bar{f}$, each of them is a convolution of quark distributions, polarization fragmentation function, and other kinematic factors originating from the eq scattering, etc. Using the parton distributions from PDFLIB [39], the perturbative calculation results for the differential cross section for $eq \to eq$, and the parametrization for the fragmentation functions, we can in principle calculate the contribution in a straightforward manner. However, in view of the number of different flavor f and $\bar{f}$ involved, all the different decay contributions and the difficulties and/or uncertainties in obtaining the fragmentation functions, the calculations are almost impossible without radical approximations. On the other hand, all this information for unpolarized reactions is implemented in the Monte-Carlo event generators such as LEPTO [43] so that the corresponding unpolarized cross section can be calculated conveniently using such Monte-Carlo programs. Such Monte-Carlo event generators have been developed since the 1980s and have been tested by enormous amount of unpolarized experiments and the parameters in the models have been adjusted to fit all the data. They provide a useful tool to make predictions for outcoming experiments and are widely used in the community. The Monte-Carlo event generators for unpolarized high energy reactions have also been used to calculate the corresponding unpolarized parts in calculating the polarizations of the produced hadrons in literature [9–22].

To show how this is carried out, we take the polarization of H in the case of $P_T = 0$ as an example and rewrite Eq. (3) as

$$P_H(z|P_T = 0) = \frac{\sum_{f,\alpha} e_f^2 \int dxdy P_b D_L(y) K(x, y) q_f(x) D_f^{H(\alpha)}(z) S_f^{H(\alpha)}}{\sum_f e_f^2 \int dxdy K(x, y)[q_f(x) D_f^H(z) + \bar{q}_f(x) D_{\bar{f}}^H(z)]}, \tag{54}$$

where $\alpha = A$ through D denoting the different origins of H: (A) directly produced and contain q_f; (B) directly produced but do not contain q_f; (C) decay product of H_j which is directly produced and contain q_f; (D) decay product of H_j which is directly produced and do not contain q_f. $S_f^{H(\alpha)} = \Delta D_f^{H(\alpha)}(z)/D_f^{H(\alpha)}(z)$ is the spin transfer factor in fragmentation for each

contribution. We see from Eqs. (32), (35), and (39) that $S_f^{H(A)} = t_{H,f}^F$, $S_f^{H(C)} = t_{H_j,f}^F t_{H,H_j}^D$ and $S_f^{H(B)} = S_f^{H(D)} = 0$. Denote the relative contribution from origin (α) by

$$R_f^{H(\alpha)}(x, y, z) = \frac{e_f^2 K(x, y) q_f(x) D_f^{H(\alpha)}(z)}{\sum_f e_f^2 \int dxdy K(x, y)[q_f(x) D_f^H(z) + \bar{q}_f(x) D_{\bar{f}}^H(z)]}, \tag{55}$$

and we have

$$P_H(z|P_T = 0) = \sum_{f,\alpha} \int dxdy R_f^{H(\alpha)}(x, y, z) P_b D_L(y) S_f^{H(\alpha)}. \tag{56}$$

We see that the relative production weight $R_f^{H(\alpha)}(x, y, z)$ defined in Eq. (55) is independent of the polarization and can be calculated using a Monte-Carlo event generator. In the right-hand side of Eq. (56), the quark polarization $P_b D_L(y)$ and the spin transfer constant $S_f^{H(\alpha)}$ are two known quantities and they are the places where information on polarization comes in. In practice, we generate a ep collision event using an event generator. We study the final state hadrons and search for the hyperon H under study. After we find a H in the considered kinematic region, we calculate $D_L(y)$ and $S_f^{H(\alpha)}$ by tracing back the origin of the H using information recorded in the Monte-Carlo program.

Usually a Monte-Carlo event generator is tested by the existing data at different energies, and is expected that it can give a reasonable description of the unpolarized quantities at a given energy provided that the physics does not have sudden changes at that energy. We therefore use such an Monte-Carlo event generator for such analysis in the following. Such a calculation method is not only the most convenient way available currently of calculating the fragmentation functions and the contributions from different hard scattering processes but also the most convenient way to include the contributions from all different decay processes.

F. A lower energy effect

At lower energies, there is another effect that relates to the valence quark contribution and may cause a difference between P_H and $P_{\bar{H}}$ in $e^- + N \to e^- + H(\text{or } \bar{H}) + X$, i.e., the contribution from the hadronization of the remnant of target nucleon. It has been pointed out first in [13] that contribution of the hadronization of target remnant is important to hyperon production even for reasonably large x_F at lower energies. (Here, $x_F \equiv 2p_\parallel/W$ is the Feynman x in the c.m. frame of the $\gamma^* p$ system, W is the total c.m. energy of the $\gamma^* p$ system. x_F is approximately equal to z at high energy W and small transverse momentum p_T [44]). The effect has been confirmed by the calculations presented in [21]. It has been shown that [13] at the CERN NOMAD energies, contributions from the hadronization of nucleon target remnant dominates hyperon production at x_F around zero. It is impossible to separate the contribution of the struck quark fragmentation from those of the target remnant fragmentation. In this case, the factorization theorem given in Eq. (1) is broken down and the concept of independent fragmentation is no more valid. Clearly, this effect can be different for hyperon and antihyperon production since the target remnant contribution comes mainly from the fragmentation of the valence diquark. It contributes quite differently for hyperons and antihyperons. This can have a large influence at lower energies, but the influence should vanish at high energies where current fragmentation can well be defined. As already demonstrated in Ref. [16], this low energy effect has already little influence on the results at COMPASS energy, in particular, when studying the difference between P_H and $P_{\bar{H}}$. We therefore do not consider this effect in the following text of this paper.

III. P_H AND $P_{\bar{H}}$ IN SIDIS WITH POLARIZED BEAM AND UNPOLARIZED TARGET

By using the method presented in the last section, we can calculate the polarizations of hyperon and antihyperon in SIDIS with the aid of a Monte-Carlo event generator. We use the latest version of LEPTO 6.5.1 [43] based on the Lund string fragmentation model [41] in the following. We study SIDIS with longitudinally polarized electron (muon) beam and unpolarized target in this section and make calculations of P_H and $P_{\bar{H}}$ in the case that a symmetric strange sea $s(x)$ and antisea distribution $\bar{s}(x)$ is assumed and in the case that an asymmetry between $s(x)$ and $\bar{s}(x)$ is taken into account separately.

A. Results with symmetric strange sea and antisea distributions

Our calculations in this case are made by using a parametrization of PDF's (parton distribution functions) obtained in PDFLIB where no asymmetry between strange sea and antisea distribution is taken into account. It is obvious that different sets of parametrizations of PDF's may have influence on our results of P_H and $P_{\bar{H}}$. In the following, we first present the results obtained using CTEQ2L and study the influence of different sets of parametrizations later in this section.

1. Results at COMPASS energy

To compare with the available experimental data, we first make calculations in the same kinematic region as in the COMPASS experiment [6,7], i.e., $Q^2 > 1$ GeV^2, and $0.2 < y < 0.9$ with μ beam energy of 160 GeV and beam

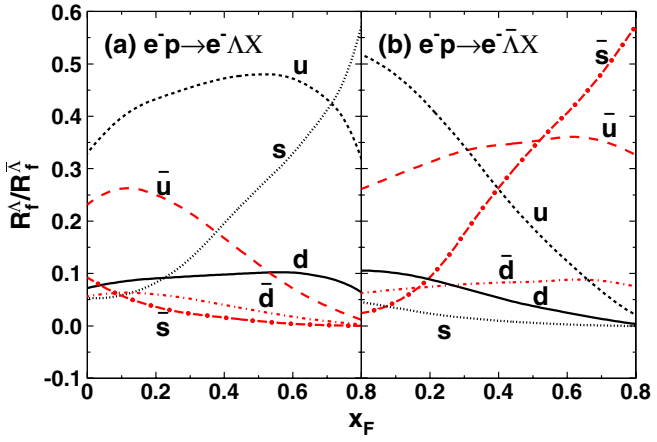

FIG. 3 (color online). Relative weights R_f^Λ and $R_f^{\bar\Lambda}$ as functions of x_F at COMPASS energy $\sqrt{s} = 17.35$ GeV for different flavors $f = u$, d, s, $\bar u$, $\bar d$, and $\bar s$, respectively.

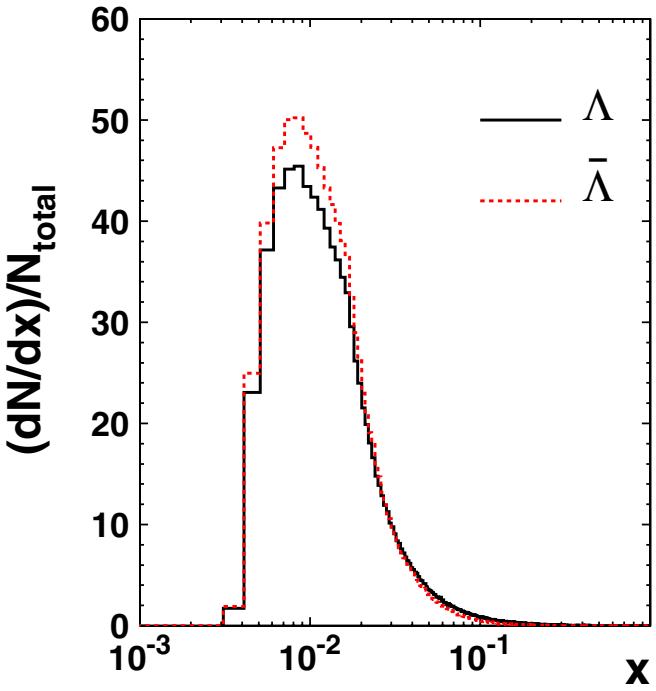

FIG. 4 (color online). The x distribution of the struck quark or antiquark that leads to the production of Λ or $\bar\Lambda$ in the kinematic region of $x_F > 0$ at COMPASS energy $\sqrt{s} = 17.35$ GeV.

polarization $P_\mu = -0.76$. As we have mentioned in the last section, when the target is unpolarized, the difference between the polarizations of H and $\bar H$ comes only from the relative weight R_f^H and $R_{\bar f}^{\bar H}$ as given by Eqs. (8) and (9). We therefore first calculated R_f^Λ and $R_f^{\bar\Lambda}$ and show the results obtained in Figs. 3(a) and 3(b), respectively. The scale for the parton distributions used in these and the following calculations in this paper is taken as the same as the momentum transfer Q in the scattering process. For comparison with experiments, we plot them as functions of x_F which is the Feynman x in the c.m. frame of the $\gamma^* p$ system and is approximately equal to z at high energy and small p_T.

From Figs. 3(a) and 3(b), we see the following features:

(1) With increasing x_F, R_s^Λ and $R_{\bar s}^{\bar\Lambda}$ increase fast, $R_{u,d}^\Lambda$ or $R_{\bar u,\bar d}^{\bar\Lambda}$ vary slowly, while $R_{\bar q}^\Lambda(x_F)$ and $R_q^{\bar\Lambda}(x_F)$ decrease, in particular, in the large x_F region. This is because $R_{u,d,s}^\Lambda$ and $R_{\bar u,\bar d,\bar s}^{\bar\Lambda}$ have the first rank contributions while $R_{u,d,s}^{\bar\Lambda}$ and $R_{\bar u,\bar d,\bar s}^\Lambda$ do not and the first rank contributions to $R_{u,d}^\Lambda$ and $R_{\bar u,\bar d}^{\bar\Lambda}$ have strangeness suppression compared to R_s^Λ and $R_{\bar s}^{\bar\Lambda}$.

(2) The shape of $R_u^\Lambda(x_F)$ is similar to $R_d^\Lambda(x_F)$ but the former is in general much larger than the latter. This is not only because of the larger contribution from the valence to u but also because the electric charge squared factor for u is 4 times as large as that for d. Similar relations hold for $\bar u$ and $\bar d$ contributions and also for those to $\bar\Lambda$.

(3) There is in general quite a large difference between R_f^Λ and $R_{\bar f}^{\bar\Lambda}$ for a given f, i.e., the charge conjugation symmetry does not hold here. The difference is particularly large for R_u^Λ and $R_{\bar u}^{\bar\Lambda}$. This is a characteristic of the contribution from the valence quark.

To understand that the valence quark contributions are still large at COMPASS energy, Ref. [16] has calculated the x values of the struck quark and/or antiquark. We did similar calculations in exactly the same COMPASS kinematic region as described above and obtain the results shown in Fig. 4. We see that most of the Λ's and $\bar\Lambda$'s are from the quark and antiquark with momentum fraction x around 0.01. In this x region, the valence quark contributions are indeed still quite large so that $u(x) > \bar u(x)$ and $d(x) > \bar d(x)$. This leads to much larger u (d) contributions to Λ than the corresponding $\bar u$ ($\bar d$) contribution to $\bar\Lambda$.

We recall that the spin transfer in fragmentation $S_f^\Lambda = S_{\bar f}^{\bar\Lambda}$ is quite different for $f = u$ or d from that for $f = s$ (see Fig. 2); we thus expect that there is a significant difference between P_Λ and $P_{\bar\Lambda}$. We calculate these polarizations using the spin transfer $S_f^\Lambda(z) = S_{\bar f}^{\bar\Lambda}(z)$ described in the last section, and show the results in Fig. 5. We see that there are indeed some differences between P_Λ and $P_{\bar\Lambda}$ at the same x_F. The magnitude of $P_{\bar\Lambda}$ is larger than that of P_Λ. This is because the contribution from the u quark is larger and S_u^Λ is small and negative.

To compare with the data from COMPASS [6,7], we also calculate the spin transfer S_{ep}^Λ and $S_{ep}^{\bar\Lambda}$ in $e^- + p \to e^- + \Lambda(\bar\Lambda) + X$ as given by Eq. (24) and show the results in Fig. 6. We recall that the magnitude of the spin transfer of s ($\bar s$) quark to Λ ($\bar\Lambda$) in the fragmentation process is much larger than that of u or d ($\bar u$ or $\bar d$) quark (see Fig. 2), so S_{ep}^Λ

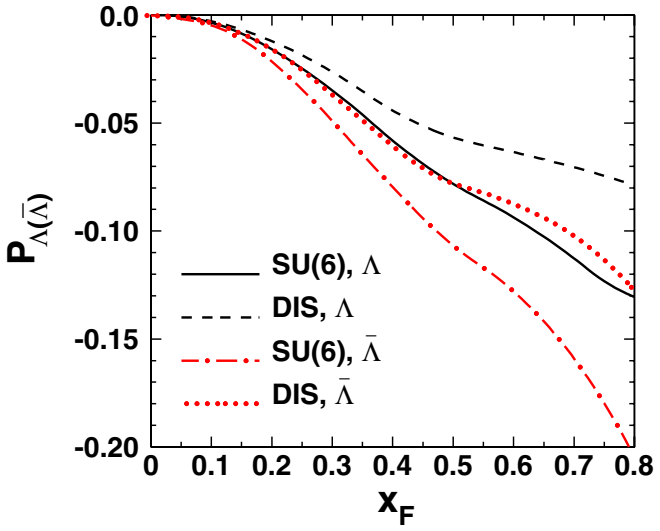

FIG. 5 (color online). Polarizations of Λ and $\bar{\Lambda}$ as the functions of x_F in SIDIS with a beam polarization of $P_b = -0.76$ at COMPASS energy $\sqrt{s} = 17.35$ GeV. These results are obtained using symmetric strange sea and antisea distributions.

$(S_{ep}^{\bar{\Lambda}})$ takes its maximum when there is only a contribution from strange quarks, i.e., $S_{ep}^{\Lambda} \to S_s^{\Lambda}$. In contrast, S_{ep}^{Λ} $(S_{ep}^{\bar{\Lambda}})$ reaches its minimum when there is only a contribution from u and/or d ($\bar{u}$ and/or $\bar{d}$), i.e., $S_{ep}^{\Lambda} \to S_u^{\Lambda} = S_d^{\Lambda}$. These are the limits of S_{ep}^{Λ} and $S_{ep}^{\bar{\Lambda}}$ in $e^- + p \to e^- + \Lambda(\bar{\Lambda}) + X$. To show the range of S_{ep}^{Λ} and $S_{ep}^{\bar{\Lambda}}$ in the case that the spin transfer model described in Sec. II D is used, we also show these two limits in the same figure.

From Fig. 6, we see that, with a symmetric strange sea and antisea distribution, we still obtain some differences between S_{ep}^{Λ} and $S_{ep}^{\bar{\Lambda}}$ as functions of x_F. But the differences seem not as large as those observed by the COMPASS

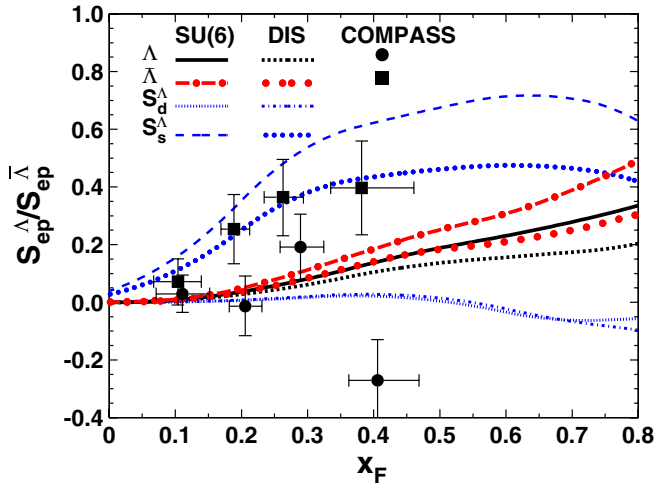

FIG. 6 (color online). Spin transfer $S_{ep}^{\Lambda/\bar{\Lambda}}$ as a function of x_F at COMPASS energy $\sqrt{s} = 17.35$ GeV obtained using symmetric strange sea and antisea distributions. The data points are taken from COMPASS [7].

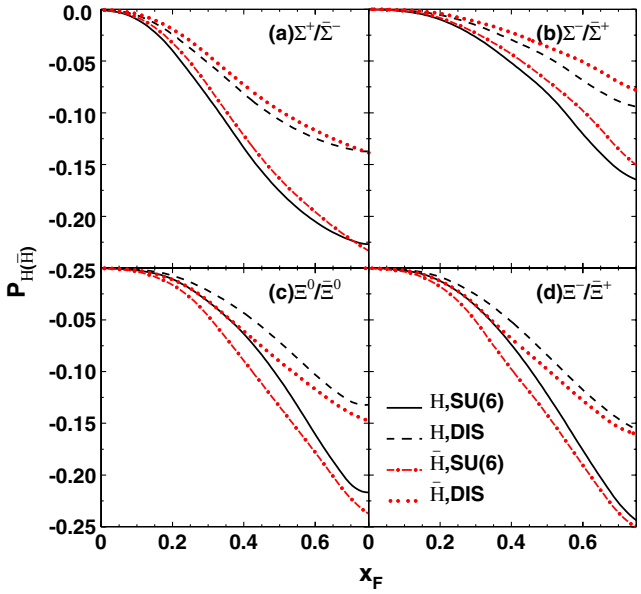

FIG. 7 (color online). Polarizations of hyperons and antihyperons as the functions of x_F in SIDIS with a beam polarization of $P_b = -0.76$ at COMPASS energy $\sqrt{s} = 17.35$ GeV. These results are obtained using symmetric strange sea and antisea distributions.

collaboration [6,7]. From the limits S_s^{Λ} and S_u^{Λ}, we see also that there is enough room to fit the data by adjusting the relative weights of s $(\bar{s})$ contributions compared to those from u and d ($\bar{u}$ and $\bar{d}$).

We have seen that the differences between P_{Λ} and $P_{\bar{\Lambda}}$ in the case discussed in this subsection come only from valence quark contributions. This is because the relative contribution from s to Λ is different from the relative contribution from $\bar{s}$ to $\bar{\Lambda}$. If we extend the study to other $J^P = (1/2)^+$ hyperons such as $\Sigma^{\pm}$ and Ξ, the situations can be different. For example, for Σ^+ and its antiparticle $\bar{\Sigma}^-$, the production and the polarization are dominated by u and $\bar{u}$ contributions, respectively. Although valence quark contributions make u dominance even stronger, the relative weights do not change much, even at COMPASS energy. Similarly, Σ^- and $\bar{\Sigma}^+$ are dominated by d and $\bar{d}$, and Ξ and $\bar{\Xi}$ are dominated by s and $\bar{s}$, respectively. We expect a much smaller difference between P_H and $P_{\bar{H}}$ for these hyperons. In Fig. 7, we show the corresponding results at COMPASS energy. We see that the differences obtained between P_H and $P_{\bar{H}}$ are indeed much smaller than those for Λ and $\bar{\Lambda}$. Since the decay contributions to these hyperons are almost negligible, the calculations here are simpler and more clear. This provides a rather clean test to see whether the difference between P_{Λ} and $P_{\bar{\Lambda}}$ is due to valence contributions.

2. Results at eRHIC energy

It is also clear that, if we go to even higher energies, the main contributions are from an even smaller x region. In

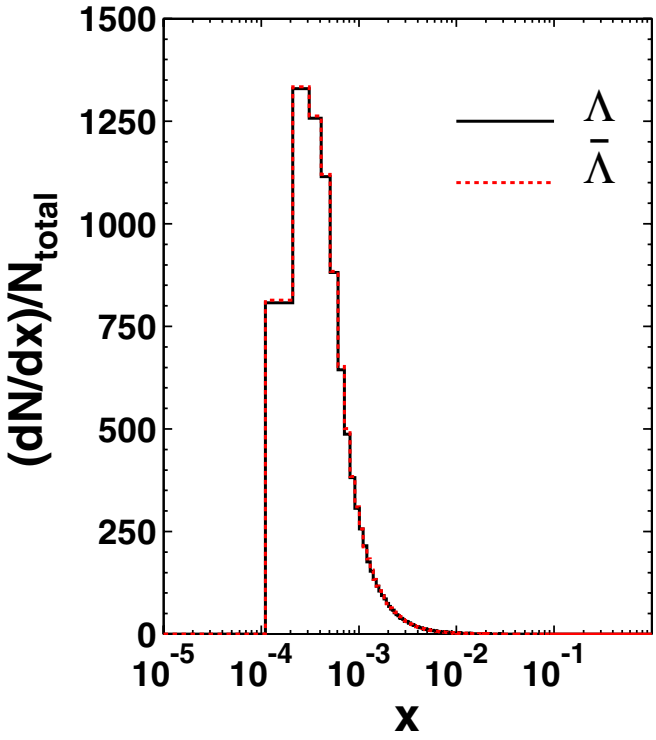

FIG. 8 (color online). The x distribution of the struck quark or antiquark that leads to the production of Λ or $\bar{\Lambda}$ in the kinematic region $x_F > 0$ at eRHIC energy $\sqrt{s} = 100$ GeV.

the small x regions, valence quark contributions are negligible. In such cases, we should have $P_H = P_{\bar{H}}$ assuming a symmetric sea and antisea quark distribution. To show this, we made calculations at eRHIC energy, i.e., we take the electron beam of 10 GeV and proton beam of 250 GeV. The electron beam polarization is taken as one and the nucleon is taken as unpolarized. We first checked the x distribution of the struck quarks (antiquarks) that lead to the productions of hyperons at such high energy. In the calculations, we choose events in the kinematic region $0.2 \leq y \leq 0.9$ and $Q^2 > 1$ GeV^2. The results are shown in Fig. 8. We see that they are indeed dominated by very small x. The results of hyperon and antihyperon polarization, using the same parton distribution set CTEQ2L with symmetric sea and antisea densities, are shown in Fig. 9. As expected, the H and $\bar{H}$ polarizations are almost the same.

3. Results obtained using different sets of PDF's

In the calculations presented above, we used CTEQ2L for parton distributions. As mentioned earlier, there are different sets of parametrizations available and the significant differences still exist for sea quark distributions especially for the strange sea. As an example, we show in Fig. 10 the s ($\bar{s}$) quark distribution in CTEQ2L and GRV98Lo. We see that the difference between the two parametrizations is indeed quite large.

The difference in different sets of PDF's can certainly influence the results of P_H and $P_{\bar{H}}$. We study this influence by repeating the calculations mentioned above using different sets of parton distribution functions. As examples, we show the results for Λ, Ξ^0, and their antiparticles in Figs. 11(a)–11(d) at COMPASS and eRHIC energies, respectively.

From the results, we indeed see some significant differences between the results obtained using the two different sets of PDF's. We see in particular that, at the COMPASS energy, the magnitude of the polarizations obtained using

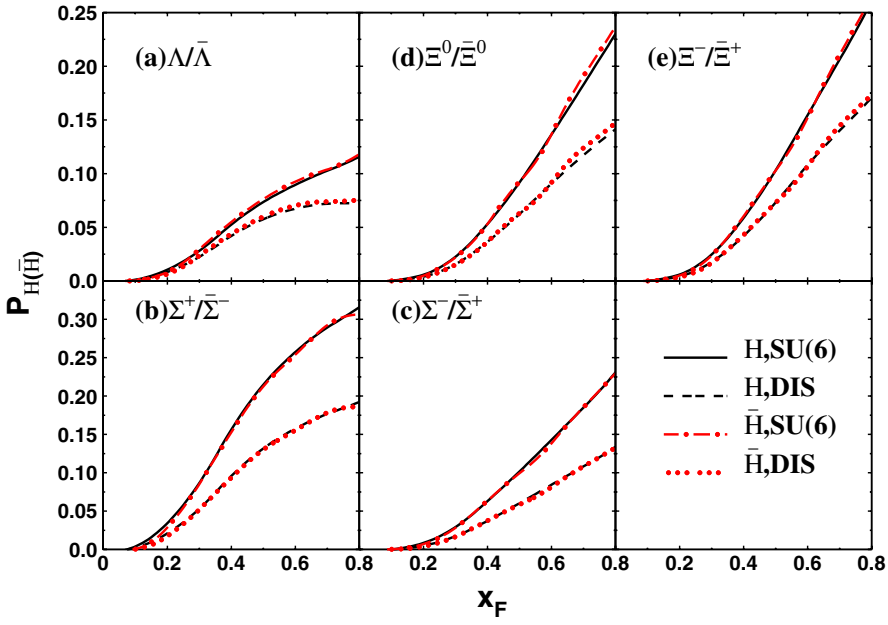

FIG. 9 (color online). Polarizations of hyperons and antihyperons as functions of x_F in SIDIS with a beam polarization of $P_b = 1$ and at eRHIC energy $\sqrt{s} = 100.0$ GeV. The results are obtained using a symmetric strange sea and antisea distribution.

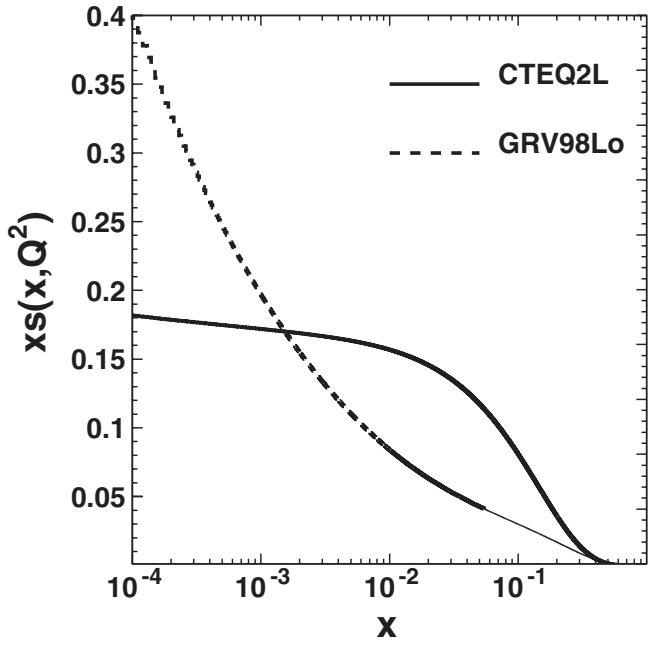

FIG. 10. Comparison of the sea quark distributions from GRV98Lo with those from CTEQ2L at $Q^2 = 3$ GeV^2.

CTEQ2L PDF's are larger than the corresponding results obtained using GRV98Lo. In contrast, at the eRHIC energy, the polarizations obtained using GRV98Lo PDF's are larger. This is because, at eRHIC energy, the dominating contributions are from the very small x region where $s(x)$ in GRV98Lo is larger than that in CTEQ2L (see Fig. 10). However, at COMPASS energy, the dominating contributions are from the much larger x region, where $s(x)$ in GRV98Lo is smaller than that in CTEQ2L. Such differences lead to different relative weights R_f^H and manifest themselves in the results for P_H and $P_{\bar{H}}$ shown in Figs. 11(a)–11(d). We also see that different sets of PDF's influence the magnitudes of P_H and $P_{\bar{H}}$ but they have little influence on the difference between them. The difference between P_H and $P_{\bar{H}}$ is not very sensitive to the parametrizations of PDF's.

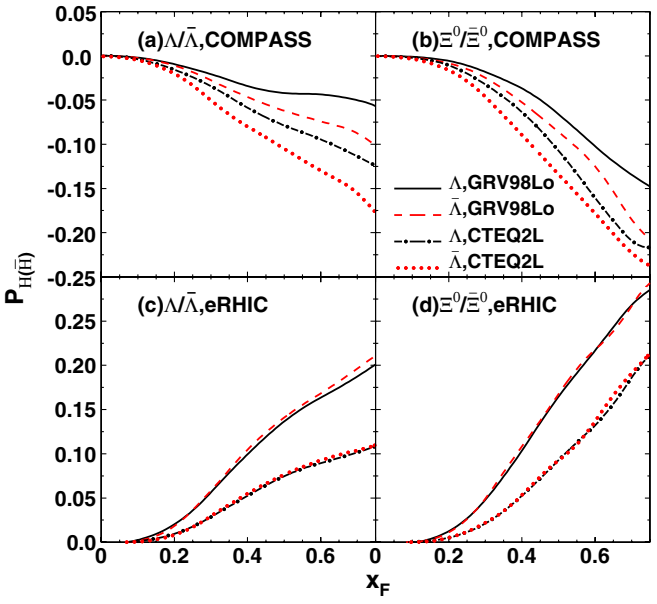

FIG. 11 (color online). Comparison of the polarizations of hyperons and antihyperons obtained using GRV98Lo with those using CTEQ2L parton distribution functions in SIDIS at the COMPASS energy (with a beam polarization of $P_b = -0.76$) and at the eRHIC energy (with $P_b = 1$), respectively. For clarity, we only show the results obtained using SU(6) picture for spin transfer in fragmentation processes.

B. Results with asymmetric strange sea and antisea distribution

As discussed in the last section, an asymmetry between strange sea and antisea quark distributions can be another source for the difference between hyperon and antihyperon polarization, and this effect remains at even higher energies such as at eRHIC. The asymmetry in the strange sea of the nucleon was studied by many authors in literature [29–34]. Different models are proposed. A global QCD fit to the CCFR and NUTEV dimuon data has also shown clear evidence that $s(x) \neq \bar{s}(x)$ [35,36], and a parametrization of the strangeness asymmetry has also been included in the CTEQ parametrization. Such an asymmetry is usually described by defining $s^-(x) = s(x) - \bar{s}(x)$, and correspondingly denoting $s^+(x) = s(x) + \bar{s}(x)$. It seems now evident that $s^-(x) \neq 0$ but the size is quite unknown. What we are sure is just the limit $-s^+(x) \leq s^-(x) \leq s^+(x)$. For example, we show two different parametriza-

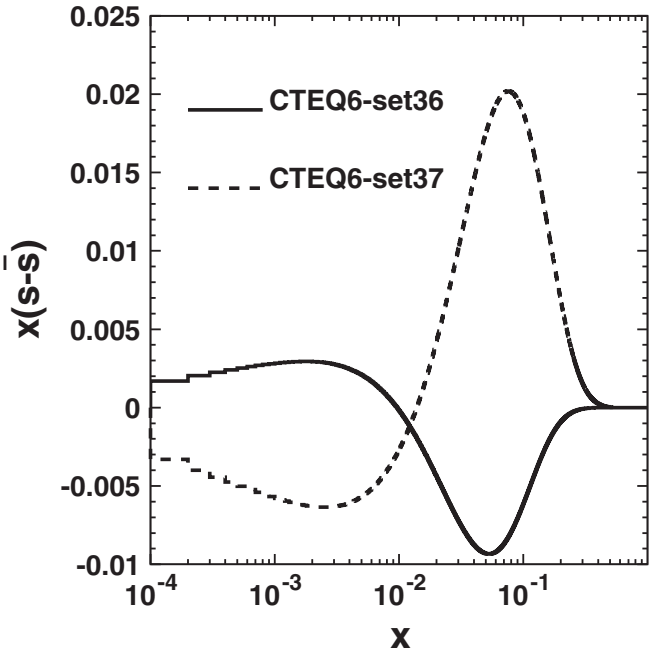

FIG. 12. Examples of the asymmetry of strangeness distributions in CTEQ6 parametrizations at $Q^2 = 3$ GeV^2. We see, in particular, that they have opposite signs in most of the x region.

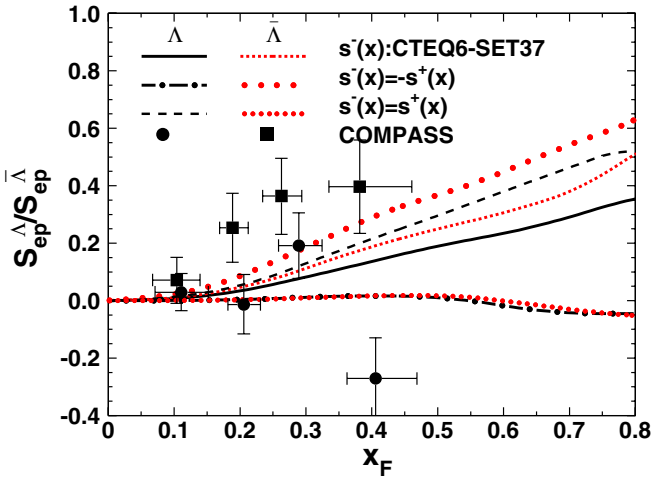

FIG. 13 (color online). Spin transfer S_{ep}^{Λ} and $S_{ep}^{\bar{\Lambda}}$ as the functions of x_F at the COMPASS energy $\sqrt{s} = 17.35$ GeV obtained using an asymmetric strangeness distribution in nucleon. Other PDF's are taken from the CTEQ2L and SU(6) picture for spin transfer in the fragmentation process are used. The data points are taken from COMPASS [7].

tions from CETQ in Fig. 12. We see that the difference in the parametrizations of $s^-(x)$ is indeed very large. We even do not know the sign of $s^-(x)$ in a given x region. In this subsection, we study the contribution of such an asymmetry to the difference between the polarization of H and that of the corresponding $\bar{H}$ in SIDIS.

We first carried out the calculations by taking the same $s^+(x)$ and other PDF's from CTEQ2L as those used in the previous calculations but taking a nonzero $s^-(x)$ into account. Since our current knowledge of $s^-(x)$ is very much limited, the form of $s^-(x)$ is almost completely unknown. We simply take an existing parametrization such as the one in CETQ6set37 for illustration. With these inputs, we obtain the Λ and $\bar{\Lambda}$ polarizations and S_{ep}^{Λ} and $S_{ep}^{\bar{\Lambda}}$ in the COMPASS kinematic region and show the results in Fig. 13. We see that, in this kinematic region, the influence from such a small asymmetry $s^-(x)$ is small. To see how large the effect can be, we consider the two extreme cases for $s^-(x)$, i.e. $s^-(x) = -s^+(x)$ or $s^-(x) = s^+(x)$. The results obtained are also shown in Fig. 13. We see that the difference between Λ and $\bar{\Lambda}$ obtained in either limit is

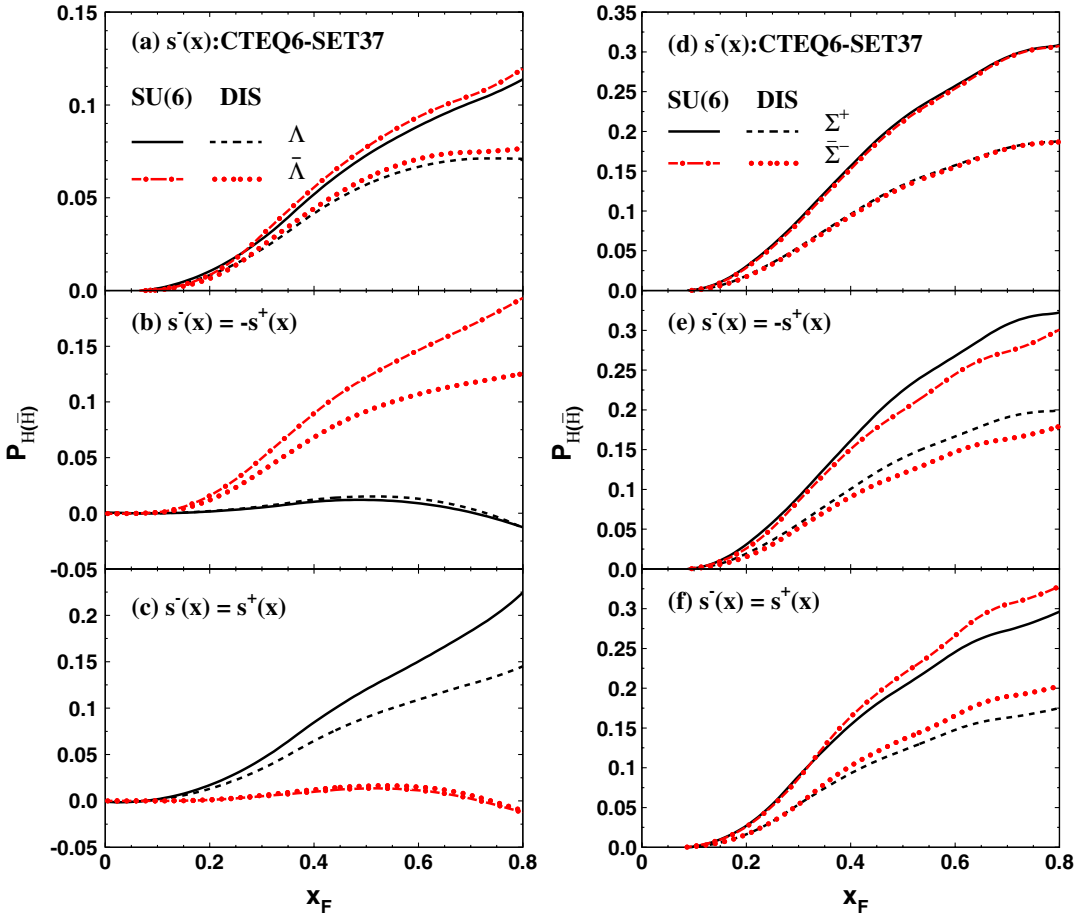

FIG. 14 (color online). Longitudinal polarizations of Λ, Σ^+, and their antiparticles obtained using different asymmetric strangeness distributions in nucleon at eRHIC energy.

much larger than that obtained in the case using a symmetric $s(x)$ and $\bar{s}(x)$ and the differences in these two limiting cases are opposite to each other. We see also that the results obtained in the limiting case that $s^-(x) = -s^+(x)$ seem to be closer to the existing COMPASS data [6,7] while those obtained in the case that $s^-(x) = s^+(x)$ seem to be in the wrong direction.

At the eRHIC energy, the only source for the difference between P_Λ and $P_{\bar{\Lambda}}$ is the asymmetry between $s(x)$ and $\bar{s}(x)$. We did similar calculations and obtain the results shown in Fig. 14. We can see that the difference between P_Λ and $P_{\bar{\Lambda}}$ is quite small if we use the asymmetric strangeness distribution as given in CTEQ6set37. However, it can be rather large in the two extreme cases. The asymmetry between $s(x)$ and $\bar{s}(x)$ has an even smaller influence on P_Σ and that for the corresponding antiparticle. For comparison, we show the results for Σ^+ and $\bar{\Sigma}^-$ in the same figure. These results show us that experiments at eRHIC can indeed provide us useful information on the asymmetry between $s(x)$ and $\bar{s}(x)$ in nucleon, but high statistics is needed.

As a brief summary of the results presented in this section, we would like to emphasize the following. We have calculated the polarizations of hyperons and their antiparticles in SIDIS with polarized lepton beam and unpolarized target. We carried out the calculations at different energies with different inputs of parton distributions and two different cases for polarized fragmentation functions. The results show that the magnitudes of the polarizations of different hyperons or those for antihyperons depend significantly on different sets of parton distributions and on the polarized fragmentation functions. Precise measurements of these polarizations should be able to shed light, in particular, on the polarized fragmentation functions. The results show also that the difference between the polarization of hyperon and that of the corresponding antihyperon depends quite weakly on different sets of parton distribution and/or fragmentation functions. These factors have significant influences on the magnitudes of the polarizations but little on the difference between the results for hyperon and those for the antihyperon. This implies that, although it is difficult to extract detailed information on the difference between sea and antisea distribution in nucleon from the difference between hyperon and antihyperon polarization since they are complicated convolutions of the different factors involved in the scattering, a significant difference at high energy such as at eRHIC can be considered as a clear signature for the existence of the difference between sea and antisea distributions in nucleon thus shed light on the fine structure of nucleon sea.

IV. P_H AND $P_{\bar{H}}$ IN SIDIS WITH UNPOLARIZED BEAM AND POLARIZED TARGET

If the lepton beam is unpolarized and the target proton is polarized with $P_T = 1$, the polarizations of the hyperons (or antihyperons) are determined by Eq. (28). In this case, the relative weights for the contributions of different flavors are the same as those discussed in the last section which are determined by the unpolarized quantities. However, the polarizations of the quarks and antiquarks are different. In the case of unpolarized lepton beam and longitudinally polarized nucleon, the polarizations of the quarks and antiquarks are equal to those in the polarized nucleon, which is a simple result of helicity conservation. This is a good place to study polarized quark distributions in the nucleon. There exist many different sets of parametrizations of the polarized PDF's [see e.g. [45–50]] and the differences between them are quite large. An example is given in Fig. 15 where two sets of parametrizations from GRSV2000 [45], GRSV2000 set3 (standard), and set4 (valence) are shown. We make calculations of P_H and $P_{\bar{H}}$ using these two sets of parametrizations of the polarized PDF's to see the sensitivity of the results of P_H and $P_{\bar{H}}$ on the polarized PDF's. We carried out the calculations in the COMPASS kinematic region and at eRHIC energy. The results at the two energies are similar and those at COMPASS energy are shown in Ref. [16]. We show those at eRHIC energy in Fig. 16.

The results show in particular following interesting features. First, the polarizations of hyperons and antihyperons

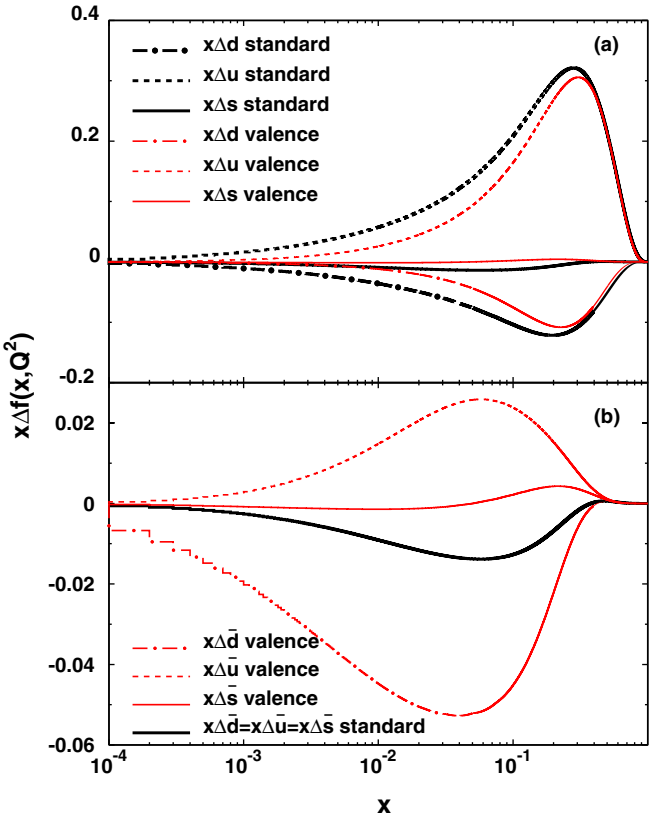

FIG. 15 (color online). Comparison of the polarized quark (a) and antiquark (b) distributions obtained from leading order GRSV2000 standard and valence scenarios at $Q^2 = 3$ GeV^2.

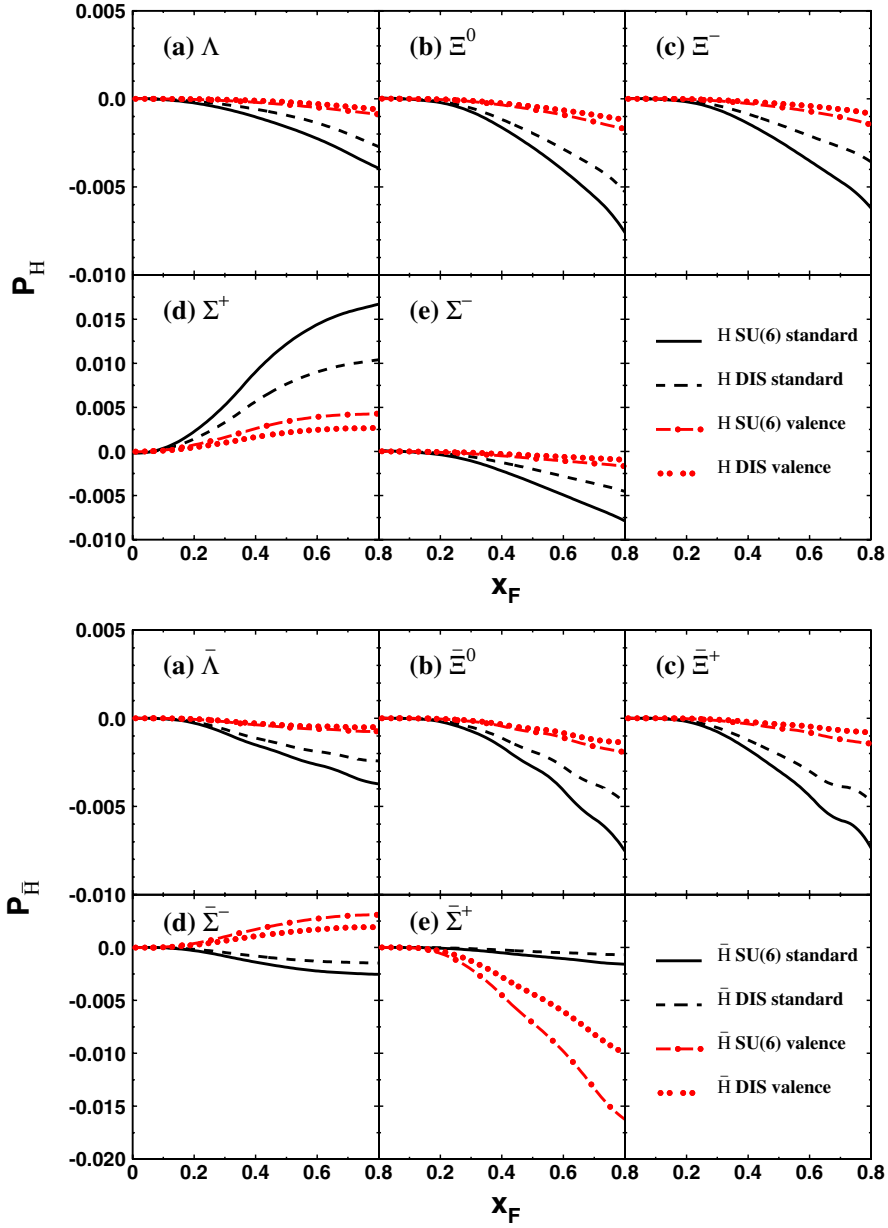

FIG. 16 (color online). Longitudinal polarizations of the hyperons (upper) and antihyperons (lower) as the functions of x_F at eRHIC energy with the longitudinal polarized target.

are quite sensitive to the polarized PDF's. Different sets of polarized PDF's lead indeed to quite different results of hyperon and antihyperon polarizations. We see, in particular, that the differences obtained from a different set of polarized PDF's are generally larger than the differences between the results for different models for the spin transfer in fragmentation. Second, because the relative weights R_f^H and spin transfer S_f^H are quite different from each other for different flavor f for a given hyperon H, the polarizations of different hyperons and antihyperons are sensitive to polarized PDF's of different flavors. For example, P_{Σ^+} and P_{Σ^-} are sensitive to $\Delta u(x)$ and $\Delta d(x)$, respectively. They have different signs because the sign of $\Delta u(x)$ is different from that of $\Delta d(x)$. The magnitude of P_{Σ^+} is larger than P_{Σ^-} because $|\Delta u(x)| > |\Delta d(x)|$. Similar features can be seen for Ξ^0, Ξ^-, and the corresponding antihyperons. These two features are important because they show that we can use hyperon polarizations in SIDIS to extract information on polarized PDF's.

V. SUMMARY AND OUTLOOK

In summary, we have calculated the longitudinal polarizations of the hyperons and antihyperons in semi-inclusive deep-inelastic scattering at COMPASS and eRHIC ener-

gies. We have, in particular, made a systematic study of the different contributions to the differences between the polarization of a hyperon and its antiparticle. We presented the results obtained in SIDIS with polarized beam and unpolarized target for the case that a symmetric strange sea and antisea distribution is used and those obtained in the case that an asymmetry between strange sea and antisea distribution is taken into account and for reactions with unpolarized beam and polarized target. Our results show that (1) at COMPASS energy, valence contributions play an important role in the difference between hyperon and antihyperon polarization but are negligible at eRHIC energy; (2) a significant asymmetry between strange sea and antisea distributions can manifest itself in the difference between hyperon and antihyperon polarization at eRHIC energy, but high statistics is needed in order to detect it; (3) different sets of PDF parametrizations have a quite large influence on the magnitudes of hyperon polarizations but the influence on the difference between hyperon and antihyperon polarization is relatively small; (4) hyperon and antihyperon polarizations in reactions using unpolarized beam and polarized target are sensitive to the polarized parton distributions and different hyperons are sensitive to different flavors, and hence can be used to extract information on flavor tagging. These results show that both the difference between hyperon and antihyperon polarization in reaction with polarized beam and unpolarized target and the polarizations of hyperons and antihyperons in reactions with unpolarized beam and polarized target are sensitive to the fine structure of the nucleon sea. Because there are many different influences from different factors involved in the scattering and the polarizations of hyperons and/or antihyperons are complicated convolutions of them, it is difficult to extract detailed information on the difference between sea and antisea quark distributions in nucleon from the difference between hyperon and antihyperon polarization in SIDIS. However, high precision measurements, in particular those at high energies such as at eRHIC, are able to provide us deep insights into the nucleon sea.

ACKNOWLEDGMENTS

This work was supported in part by the National Natural Science Foundation of China under the approval No. 10525523 and Department of Science and Technology of Shandong Province.

[1] D. Buskulic *et al.* (ALEPH Collaboration), Phys. Lett. B **374**, 319 (1996).
[2] K. Ackerstaff *et al.* (OPAL Collaboration), Eur. Phys. J. C **2**, 49 (1998).
[3] P. Astier *et al.* (NOMAD Collaboration), Nucl. Phys. **B588**, 3 (2000); **B605**, 3 (2001).
[4] M. R. Adams *et al.* (E665 Collaboration), Eur. Phys. J. C **17**, 263 (2000).
[5] A. Airapetian *et al.* (HERMES Collaboration), Phys. Rev. D **64**, 112005 (2001); **74**, 072004 (2006).
[6] V. Y. Alexakhin (COMPASS Collaboration), arXiv:hep-ex/0502014.
[7] M. G. Sapozhnikov (COMPASS Collaboration), arXiv: hep-ex/0503009; arXiv:hep-ex/0602002; International Workshop on Hadron Structure and QCD (HSQCD'2008), Gatchina, Russia, 2008.
[8] Q. H. Xu (STAR Collaboration), AIP Conf. Proc. **842**, 71 (2006); **915**, 428 (2007); E. P. Sichtermann (STAR Collaboration), 18th International Symposium on Spin Physics, University of Virginia, 2008.
[9] G. Gustafson and J. Hakkinen, Phys. Lett. B **303**, 350 (1993).
[10] C. Boros and Z. T. Liang, Phys. Rev. D **57**, 4491 (1998).
[11] C. X. Liu and Z. T. Liang, Phys. Rev. D **62**, 094001 (2000).
[12] C. X. Liu, Q. H. Xu, and Z. T. Liang, Phys. Rev. D **64**, 073004 (2001).
[13] Z. T. Liang, in *Proceedings of the 31st International Symposium on Multiparticle Dynamics (ISMD 2001), Datong, China*, edited by Wu *et al.* (World Scientific, Singapore, 2001), pp. 78–83; Z. T. Liang and C. X. Liu, Phys. Rev. D **66**, 057302 (2002).
[14] Q. H. Xu, C. X. Liu, and Z. T. Liang, Phys. Rev. D **65**, 114008 (2002).
[15] Q. H. Xu and Z. T. Liang, Phys. Rev. D **70**, 034015 (2004).
[16] H. Dong, J. Zhou, and Z. T. Liang, Phys. Rev. D **72**, 033006 (2005).
[17] Q. H. Xu, Z. T. Liang, and E. Sichtermann, Phys. Rev. D **73**, 077503 (2006).
[18] Y. Chen, Z. T. Liang, E. Sichtermann, Q. H. Xu, and S. S. Zhou, Phys. Rev. D **78**, 054007 (2008).
[19] J. R. Ellis, D. Kharzeev, and A. Kotzinian, Z. Phys. C **69**, 467 (1996).
[20] A. Kotzinian, A. Bravar, and D. von Harrach, Eur. Phys. J. C **2**, 329 (1998).
[21] J. R. Ellis, A. Kotzinian, and D. Naumov, Eur. Phys. J. C **25**, 603 (2002).
[22] J. R. Ellis, A. Kotzinian, D. Naumov, and M. Sapozhnikov, Eur. Phys. J. C **52**, 283 (2007).
[23] B. Q. Ma and J. Soffer, Phys. Rev. Lett. **82**, 2250 (1999).
[24] B. Q. Ma, I. Schmidt, J. Soffer, and J. J. Yang, Phys. Rev. D **62**, 114009 (2000).
[25] B. Q. Ma, I. Schmidt, J. Soffer, and J. J. Yang, Eur. Phys. J. C **16**, 657 (2000).
[26] B. Q. Ma, I. Schmidt, J. Soffer, and J. J. Yang, Phys. Lett. B **488**, 254 (2000).
[27] M. Anselmino, M. Boglione, and F. Murgia, Phys. Lett. B **481**, 253 (2000).

[28] M. Anselmino, M. Boglione, U. D'Alesio, E. Leader, and F. Murgia, Phys. Lett. B **509**, 246 (2001).
[29] A. I. Signal and A. W. Thomas, Phys. Lett. B **191**, 205 (1987).
[30] S. J. Brodsky and B. Q. Ma, Phys. Lett. B **381**, 317 (1996).
[31] M. Burkardt and B. Warr, Phys. Rev. D **45**, 958 (1992).
[32] H. Holtmann, A. Szczurek, and J. Speth, Nucl. Phys. **A596**, 631 (1996).
[33] H. R. Christiansen and J. Magnin, Phys. Lett. B **445**, 8 (1998).
[34] F. G. Cao and A. I. Signal, Phys. Rev. D **60**, 074021 (1999).
[35] F. Olness *et al.*, Eur. Phys. J. C **40**, 145 (2005).
[36] H. L. Lai, P. M. Nadolsky, J. Pumplin, D. Stump, W. K. Tung, and C. P. Yuan, J. High Energy Phys. 04 (2007) 089.
[37] A. Deshpande, R. Milner, R. Venugopalan, and W. Vogelsang, Annu. Rev. Nucl. Part. Sci. **55**, 165 (2005).
[38] B. Jager, A. Schafer, M. Stratmann, and W. Vogelsang, Phys. Rev. D **67**, 054005 (2003).
[39] H. Plothow-Besch, Comput. Phys. Commun. **75**, 396 (1993).
[40] R. D. Field and R. P. Feynman, Nucl. Phys. **B136**, 1 (1978).
[41] B. Andersson, G. Gustafson, G. Ingelman, and T. Sjostrand, Phys. Rep. **97**, 31 (1983).
[42] T. Sjostrand, Comput. Phys. Commun. **82**, 74 (1994).
[43] G. Ingelman, A. Edin, and J. Rathsman, Comput. Phys. Commun. **101**, 108 (1997).
[44] We recall that $z = 2p/W$ so the relation between z and x_F is given by $x_F = \sqrt{z^2 - 4p_\perp^2/[sy(1-x) + M^2]}$, where s is the c.m. energy squared of the ep system and M is the proton mass. The differential cross section with respect to x_F is then obtained by integrating over x, y, and z with the appropriate Jacobi determinant taken into account. In our calculations using the Monte-Carlo method described in Sec. II E with the aid of the event generator, this is taken into account automatically.
[45] M. Gluck, E. Reya, M. Stratmann, and W. Vogelsang, Phys. Rev. D **53**, 4775 (1996); **63**, 094005 (2001).
[46] J. Blumlein and H. Bottcher, Nucl. Phys. **B636**, 225 (2002).
[47] E. Leader, A. V. Sidorov, and D. B. Stamenov, Phys. Rev. D **73**, 034023 (2006); **75**, 074027 (2007).
[48] T. Gehrmann and W. J. Stirling, Phys. Rev. D **53**, 6100 (1996).
[49] M. Hirai, S. Kumano, and N. Saito (Asymmetry Analysis Collaboration), Phys. Rev. D **69**, 054021 (2004); **74**, 014015 (2006).
[50] D. de Florian and R. Sassot, Phys. Rev. D **62**, 094025 (2000); D. de Florian, G. A. Navarro, and R. Sassot, Phys. Rev. D **71**, 094018 (2005); D. de Florian, R. Sassot, M. Stratmann, and W. Vogelsang, Phys. Rev. Lett. **101**, 072001 (2008).